

# Thermal and Photolytic Reactions of Gallium and Indium Atoms (M) and Their Dimers M<sub>2</sub> with Carbon Monoxide in Low-Temperature Matrices: Formation of Terminal, Bridged, and Ionic Carbonyl Derivatives†

Hans-Jörg Himmel,\* Anthony J. Downs, Jennifer C. Green, and Tim M. Greene

Inorganic Chemistry Laboratory, University of Oxford, South Parks Road, Oxford, OX1 3QR, U.K.

Received: October 28, 1999; In Final Form: February 15, 2000

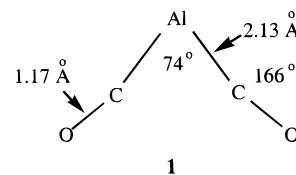
Infrared spectroscopy has been used to chart the thermal reactions occurring following co-deposition of gallium or indium vapors with carbon monoxide-doped argon at ca. 12 K, as well as the reactions subsequently induced by irradiating the resulting matrix with UV light ( $\lambda = 200\text{--}400\text{ nm}$ ). Following deposition, the molecules GaCO, InCO, Ga·GaCO, In·InCO, Ga( $\mu$ -CO)Ga, Ga(CO)<sub>2</sub>, In(CO)<sub>2</sub>, and In(CO)<sub>2</sub>·In were generated. Under the action of UV light, the Ga/CO system gives rise to the new gallium carbonyl Ga( $\mu$ -CO)<sub>2</sub>Ga. Under similar conditions, the complex In<sup>+</sup>[C<sub>2</sub>O<sub>2</sub>]<sup>-</sup> is formed as a result of significant charge transfer between the metal and the CO ligands and with the concomitant linking together of two such ligands via a C–C bond. Assignments of the absorption bands are made and the products characterized on the basis of <sup>13</sup>C substitution and by comparison with the vibrational properties of known carbonyl derivatives or with those forecast for novel species by DFT calculations.

## 1. Introduction

Among the first organometallic compounds to be prepared and studied, carbonyl derivatives represent a familiar and important body of transition-metal compounds that include the possibility of both terminal and bridging CO groups.<sup>1</sup> They are admirably suited to investigation by infrared measurements, mainly by virtue of the very intense absorptions associated with the  $\nu(\text{C}=\text{O})$  modes which they possess, and the properties of which afford sensitive measures of the geometry and bonding of M(CO)<sub>*n*</sub> fragments.<sup>2</sup> They are noteworthy too not only for the catalytic potential they offer through ready access to highly reactive unsaturated intermediates but also for their photolability which typically depends on the fission of an M–CO bond and the formation of one of these intermediates.<sup>3</sup> Their properties commend them especially to matrix-isolation studies.<sup>4</sup>

On the other hand, it was generally believed for many years that carbonyl derivatives are confined to the metals of the d-block. That main group elements are also capable of binding CO, although usually to give species that are short-lived under normal conditions, did not become apparent until the 1970s when various matrix-isolation experiments revealed that atoms as diverse as Si,<sup>5</sup> Sn,<sup>6</sup> and U<sup>7</sup> are all capable of binding CO quite specifically. The first sign that the group 13 elements share this capability came in 1972 with the report<sup>8</sup> that the matrix formed by cocondensing Al atoms with CO and an excess of krypton at 20 K displays infrared bands attributable to the aluminum dicarbonyl Al<sub>*x*</sub>(CO)<sub>2</sub>. Various studies involving different matrices and EPR<sup>9</sup> as well as IR<sup>10–13</sup> measurements have confirmed this first sighting and shown that  $x = 1$ . On the evidence of quantum chemical calculations,<sup>14</sup> the molecule has the angular structure **1** with a tight C–Al–C angle of about 74° between Al–C–O arms which are bent slightly but significantly so as to appear to draw the two carbon atoms toward each other. A total binding energy of about 70 kJ mol<sup>-1</sup> was estimated, in

good agreement with an experimental value derived from studies of the chemiluminescent oxidation of the molecules by O<sub>3</sub>.<sup>15</sup> Under appropriate conditions, the corresponding monocarbonyl AlCO has also been identified by its infrared spectrum,<sup>11–14</sup>



with results well replicated by recent ab initio calculations.<sup>16</sup> Similar methods have led to the detection and characterization of the following carbonyl derivatives of the other group 13 elements: BCO (EPR<sup>17</sup> and IR<sup>17,18</sup>), B(CO)<sub>2</sub> (IR<sup>18</sup>); Ga(CO)<sub>2</sub> (EPR<sup>19,20</sup> and IR<sup>13,20,21</sup>); and In(CO)<sub>2</sub> (EPR and IR<sup>22</sup>). In addition, infrared spectra have afforded what has been mostly circumstantial evidence suggesting the formation of the dinuclear species OCBBCO,<sup>18</sup> Al<sub>2</sub>CO,<sup>12</sup> and Al<sub>2</sub>(CO)<sub>4</sub>.<sup>12</sup> The last two of these are distinguished by  $\nu(\text{C}=\text{O})$  frequencies low enough to encourage the belief that one or more CO groups have a bridging function. Surprisingly, however, the well-known photolability of transition metal carbonyls<sup>3,4</sup> has not spurred any investigation of how these main group metal carbonyls respond to light of different wavelengths.

Here we report the results of a detailed matrix-isolation study of the thermal reactions that occur between CO molecules and gallium or indium vapors on cocondensation with an excess of argon at 12 K. The effects of UV and broad-band UV–visible photolysis on the resulting matrices have been explored. The course of events has been followed, and the products have been detected and characterized by the  $\nu(\text{C}=\text{O})$  bands in their infrared spectra, experiments with <sup>13</sup>CO serving to underpin the findings. The experimental results have been analyzed in the light of quantum chemical studies using density functional theory (DFT). The products of the thermal reactions include the mononuclear

† Part of the special issue "Marilyn Jacox Festschrift".

\* To whom correspondence should be addressed.

species MCO and  $M(\text{CO})_2$  ( $M = \text{Ga}$  or  $\text{In}$ ). The IR spectra also give evidence for the interaction of the MCO ( $M = \text{Ga}$  or  $\text{In}$ ) and  $\text{In}(\text{CO})_2$  species with an additional metal atom to yield loosely bound aggregates  $M(\text{CO})_n \cdot M$ . In addition, reactions with metal dimers  $M_2$  give rise to the dinuclear carbonyls  $\text{Ga}_2\text{CO}$ ,  $\text{In}_2\text{CO}$ , and  $\text{Ga}(\mu\text{-CO})\text{Ga}$ . UV irradiation results in the decay of these products and the formation of a new digallium derivative  $\text{Ga}(\mu\text{-CO})_2\text{Ga}$  incorporating two bridging CO groups. Under similar conditions, indium shows behavior resembling that of an alkali metal<sup>23–25</sup> with evidence of significant charge transfer to give what is essentially a derivative of the  $\text{OC-CO}^-$  ion characterized by a  $\nu(\text{C-O})$  band at the unusually low frequency of  $1515.5 \text{ cm}^{-1}$ . The carbonyls are contrasted with one another and with related derivatives on the strength of the properties they display.

## 2. Experimental Section

Gallium (Aldrich, 99.9999% pure) and indium (Aldrich, 99.999% pure) were each evaporated from a tantalum Knudsen cell which was heated to ca.  $950 \text{ }^\circ\text{C}$ . Hence the vapor was deposited with an excess of CO-doped argon on a CsI window cooled normally to  $12 \text{ K}$  by means of a Displex closed-cycle refrigerator (Air Products, model CS202). The  $^{12}\text{CO}$  was admixed with the argon (both Research Grade and used as supplied by BOC) at concentrations typically ranging from 2 to 10%.  $^{13}\text{CO}$  (99 at. %, less than 1 at. %  $^{18}\text{O}$ ) was also used as supplied, in this case by Cambridge Isotope Laboratories. Typical deposition rates were ca. 2 mmol of matrix gas per hour, continued over a period of 2–3 h.

Following deposition, the samples were exposed to the radiation from a Spectral Energy Hg–Xe arc lamp operating at 800 W. The first step typically involved photolysis for 10 min with UV light at wavelengths in the range 200–400 nm provided by means of a visible block filter (Oriel) which absorbed light in the range  $400 < \lambda < 700 \text{ nm}$  and a water filter to absorb infrared radiation. This was followed by broadband UV–visible photolysis, again for 10 min, the wavelengths now being in the range 200–800 nm with only the water filter to limit the radiation reaching the matrix.

Infrared spectra of the matrix samples were recorded at a resolution of  $0.5 \text{ cm}^{-1}$  and with an accuracy of  $\pm 0.1 \text{ cm}^{-1}$  using a Nicolet Magna-IR 560 FTIR instrument equipped with a liquid  $\text{N}_2$  cooled MCTB detector for the spectral range 4000–400  $\text{cm}^{-1}$ . The wavenumbers and relative intensities of the  $\nu(\text{C-O})$  features in the IR spectra of individual products incorporating  $M(\text{CO})_n$  fragments at varying levels of  $^{13}\text{CO}$  enrichment were calculated on the basis of an energy-factored force field using simple iterative refinement programs; IR spectra were then simulated with a program that constructed Lorentzian band shapes based on the calculated intensities.<sup>26</sup>

The calculations were carried out using the Amsterdam Density Functional (ADF) program system, version 2.3.<sup>27,28</sup> The electronic configurations of the molecular systems were described by an uncontracted triple- $\xi$  basis set of Slater-type orbitals (STO). Carbon, oxygen, and the group 13 elements were given extra polarization functions, 3d on C and O and  $(n + 1)d$  on Al, Ga, and In. The cores of the atoms were frozen, C and O up to 1s, Al up to 2p, Ga up to 3p, and In up to 4p. First-order relativistic corrections were made to the cores of all atoms using the Pauli formalism. Energies were calculated using Vosko, Wilk, and Nusair's local exchange correlation potential,<sup>29</sup> with nonlocal exchange corrections by Becke,<sup>30</sup> and nonlocal

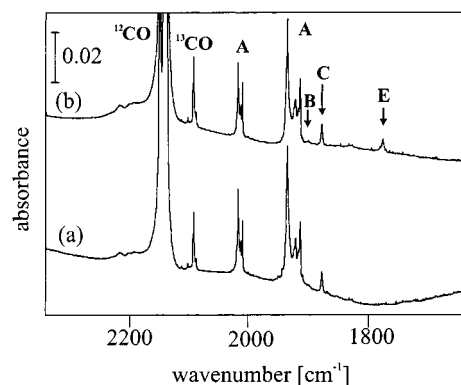


**Figure 1.** IR spectrum of an Ar matrix containing Ga and 2%  $^{12}\text{CO}$ : (a) following deposition; and (b) following UV photolysis ( $\lambda = 200\text{--}400 \text{ nm}$ ).

correlation corrections by Perdew.<sup>31</sup> Frequencies were computed by numerical differentiation of slightly displaced geometries.<sup>32,33</sup>

## 3. Results

The infrared spectra associated with the matrix-isolated products formed (i) by the thermal reactions between CO and either the metal atoms  $M$  ( $M = \text{Ga}$  or  $\text{In}$ ) or the diatomic molecules  $M_2$  and (ii) by subsequent photolytically induced changes will be reported in turn, first for gallium and then for indium. Bands have been assigned on the strength of the following criteria: (i) their growth/decay characteristics measured as a function of changes in the matrix conditions (e.g. concentrations and responses to photolysis or annealing); (ii) comparisons with the spectra of related species (e.g.  $\text{AlCO}$ ,<sup>11–13</sup>  $\text{Al}(\text{CO})_2$ ,<sup>8,10–13</sup> and  $\text{Al}(\mu\text{-CO})\text{Al}$ <sup>12</sup>); (iii) reference to the effects of total or partial  $^{13}\text{CO}$  substitution; and (iv) the extent to which the measured spectroscopic properties match those forecast by DFT calculations for a given molecule in its optimized geometry.

**Gallium.** Figure 1 illustrates the infrared spectra exhibited by a matrix formed by co-depositing gallium vapor with argon containing 2% CO at  $12 \text{ K}$ , and then irradiating the sample initially with UV light. The observed frequencies are detailed in Table 1. Following deposition, the matrix displayed significant absorptions over and above those due to free CO and its aggregates.<sup>34</sup> Systematic studies involving changes in the relative concentrations of CO and metal atoms and observation of how the absorptions grew or decayed pointed to the presence of three distinct gallium carbonyls **A**, **B**, and **C**. The principal features, associated with the product **A**, were two strong triplets with components at the following wavenumbers (in  $\text{cm}^{-1}$ ): 2016.8/2011.8/2009.2 and 1933.6/1920.4/1912.4. The spectrum included, in addition, a broad band at  $1898.1 \text{ cm}^{-1}$  and a sharp doublet with a strong signal at  $1875.6$  and a weaker one at  $1866.5 \text{ cm}^{-1}$  originating in the products **B** and **C**, respectively. The doublet pattern observed for **C** was attributed not to two different modes but to two different matrix sites. Two weak absorptions at  $1849.5$  and  $1839.9 \text{ cm}^{-1}$  were also observed, as was a weak but sharp absorption at  $1828.0 \text{ cm}^{-1}$  that was attributed to a product **D**.

Irradiation of the matrix with UV light ( $200 < \lambda < 400 \text{ nm}$ ) witnessed a decrease in the intensities of all the signals associated with the products **A**, **B**, **C**, and **D**. At the same time a new absorption was observed to grow in at the significantly lower frequency of  $1774.0 \text{ cm}^{-1}$ . None of the previous reports of gallium carbonyls contain any reference to this feature, and so we conclude that it belongs to a new species **E**, the formation of which requires photoactivation.

**TABLE 1: Infrared Absorptions Associated with the Products of the Reactions of Ga with  $^{12}\text{CO}/(^{12}\text{CO} + ^{13}\text{CO})/^{13}\text{CO}$  (Frequencies in  $\text{cm}^{-1}$ )**

Ga + $^{12}\text{CO}$	Ga + $(^{12}\text{CO} + ^{13}\text{CO})$	Ga + $^{13}\text{CO}$	increase in CO%	$\lambda = 200\text{--}400$ nm photolysis <sup>a</sup>	broad-band photolysis <sup>a</sup>	absorber
2016.8	2016.8					Ga(CO) <sub>2</sub> , <b>A</b>
2011.8	2011.8					
2009.2	2009.2					
	1999.9		↑	↓	↓	
	1991.6					
	1972.8	1972.8				Ga(CO) <sub>2</sub> , <b>A</b>
	1967.9	1967.9				
	1965.1	1965.1				
1933.6	1933.6					
1920.4	1920.4					Ga(CO) <sub>2</sub> , <b>A</b>
1912.4	1912.4					
	1907.7		↑	↓	↓	Ga(CO) <sub>2</sub> , <b>A</b>
	1892.9	1892.9				
	1880.1	1880.1				
	1872.0	1872.0				
1898.1	1898.1		↑	↓	↓	Ga·GaCO, <b>B</b>
	1857.8	1857.8				GaCO (site I), <b>C</b>
1875.6	1875.6		↓	↓	↓	
	1834.6	1834.6				GaCO (site II), <b>C</b>
1866.5	1866.5		↓	↓	-	
	1825.9	1825.9				Ga <sub>x</sub> (CO) <sub>y</sub>
1849.5	1849.7		↓	↓	↓	
	1809.3	1809.2				Ga <sub>x</sub> (CO) <sub>y</sub>
1839.9	<i>b</i>	1802.4	↓	↓	↓	
1828.0	1828.2		↓	↓	↓	Ga( $\mu$ -CO)Ga, <b>D</b>
	1789.6	1789.6				
1774.0	1774.0					Ga( $\mu$ -CO) <sub>2</sub> Ga, <b>E</b>
	1752.8		↑	↑	↓	
	1736.8	1736.8				

<sup>a</sup> ↑: increase in intensity. ↓: decrease in intensity. <sup>b</sup> Hidden by more intense absorptions.

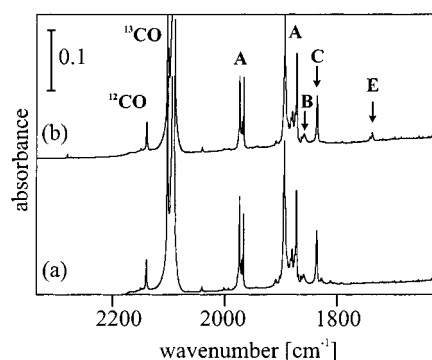


**Figure 2.** IR spectrum of an Ar matrix containing Ga and 2%  $^{13}\text{CO}$ : (a) following deposition; and (b) following UV photolysis ( $\lambda = 200\text{--}400$  nm).

There followed a period (10 min) of irradiation of the matrix with broad-band UV–visible light ( $200 < \lambda < 800$  nm). This resulted in a further diminution in the intensities of the infrared absorptions due to the products **A**, **C**, and **D** and also to the virtual extinction of the absorption due to **B**. Moreover, the absorption at  $1774.0\text{ cm}^{-1}$  which had developed on UV photolysis was totally extinguished, implying a high degree of photolability for its carrier **E**, reminiscent of that displayed by unsaturated transition-metal carbonyl species.<sup>2–4</sup>

Additional information was sought by repeating the experiments with  $^{13}\text{CO}$  in place of  $^{12}\text{CO}$ , with the results illustrated in Figure 2 and detailed in Table 1. The two triplets belonging to **A** were each seen to be shifted, the higher frequency set by ca.  $44\text{ cm}^{-1}$ , the lower frequency one by ca.  $40\text{ cm}^{-1}$ . The bands due to **B**, **C** and **D** were likewise displaced by  $40.3$ ,  $41.0/40.6$ , and  $38.2\text{ cm}^{-1}$ , respectively, that due to **E** by  $37.2\text{ cm}^{-1}$ . Hence there is every reason to believe that the bands in question correspond to  $\nu(\text{C}\text{--}\text{O})$  fundamentals of CO groups coordinated

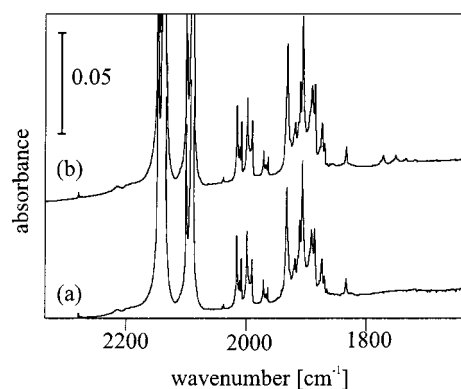


**Figure 3.** IR spectrum of an Ar matrix containing Ga and a mixture of  $^{12}\text{CO}$  and  $^{13}\text{CO}$  (2:1, total 2%): (a) following deposition; and (b) following UV photolysis ( $\lambda = 200\text{--}400$  nm).

to one or more Ga atoms. The two weak signals at  $1849.5$  and  $1839.9\text{ cm}^{-1}$  in the experiments carried out with  $^{12}\text{CO}$  were observed to be shifted to  $1809.2$  and  $1802.4\text{ cm}^{-1}$  in the case of  $^{13}\text{CO}$ .

To assess the number of such CO groups in each species, experiments were then carried out not with a single isotopomer but with a mixture of  $^{12}\text{CO}$  and  $^{13}\text{CO}$  (with  $^{12}\text{CO}:^{13}\text{CO} = \text{ca. } 2:1$ , see Figure 3 and Table 1). It appeared that each of the two features associated with **A** was split into a *triplet* pattern with relative intensities in the proportions of roughly  $2:2:1$ , signaling the presence of two symmetrically equivalent CO groups. By contrast, **B** and **D** gave only *doublets* with components corresponding to the bands observed separately in the experiments with either  $^{12}\text{CO}$  or  $^{13}\text{CO}$  alone, and so must be presumed to carry only a single CO group. After photolysis at wavelengths in the range  $\lambda = 200\text{--}400$  nm, it was found that the new product **E** was now characterized by a *triplet* of infrared bands at  $1774.0$ ,

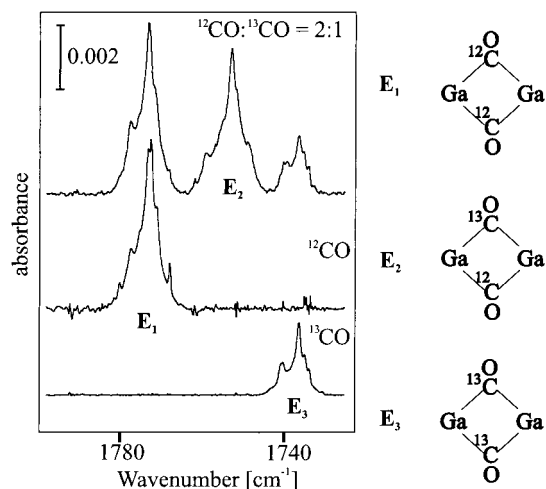


**Figure 4.** IR spectra showing the out-of-phase  $\nu(\text{C}-\text{O})$  mode of  $\text{Ga}-(\mu\text{-CO})_2\text{Ga}$  isolated in Ar matrices and formed from  $^{13}\text{CO}$ ,  $^{12}\text{CO}$ , and  $^{12}\text{CO}/^{13}\text{CO}$  (2:1 mixture).

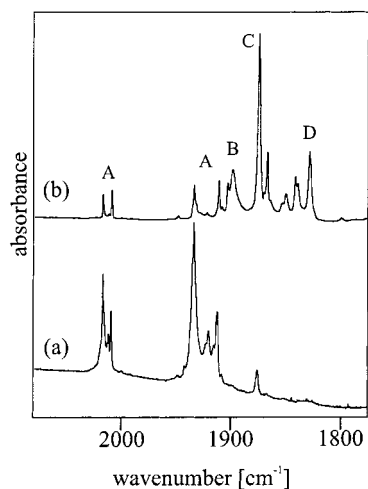


**Figure 5.** IR spectra of Ar matrices containing Ga and  $^{12}\text{CO}$  at different concentrations: (a) 2% CO; and (b) 0.2% CO.

1752.8, and 1736.8  $\text{cm}^{-1}$  (see Figure 4). It follows that **E**, like **A**, contains two symmetrically equivalent CO groups. That all the components of the triplet were indeed carried by **E** in one isotopic form or another was confirmed by their extinction following 10 min exposure of the matrix to broad-band UV-visible radiation.

Additional experiments were carried out with lower concentrations of CO. Figure 5 shows the spectrum obtained using a CO concentration of 0.2% in contrast to that observed with a CO concentration of 2%. Hence it appeared that the intensities of the two triplets associated with product **A**, previously the dominant features in the spectrum obtained for 2% CO concentration, were much reduced in the spectrum of the matrix containing 0.2% CO. Instead, the matrix showed a large increase in the intensities of the bands associated with the products **B**, **C**, and **D**.

Experiments were also carried out with a CO concentration of 2%, but using krypton as the host gas instead of argon to gain information about the origin of the triplet structure attributed to species **A**. Figure 6 compares the resulting IR spectra for both krypton and argon matrices. In the case of krypton, one of the three absorptions of each triplet dominates the spectrum, being located at 2006.1 and 1909.3  $\text{cm}^{-1}$ , respectively. This suggests that the triplet patterns found for Ar matrices originate mainly from one species and are due to

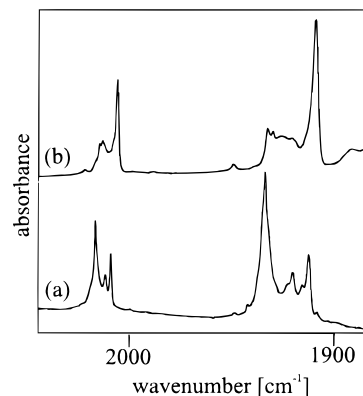


**Figure 6.** IR spectra of (a) an Ar matrix and (b) a Kr matrix containing Ga and 2%  $^{12}\text{CO}$ .

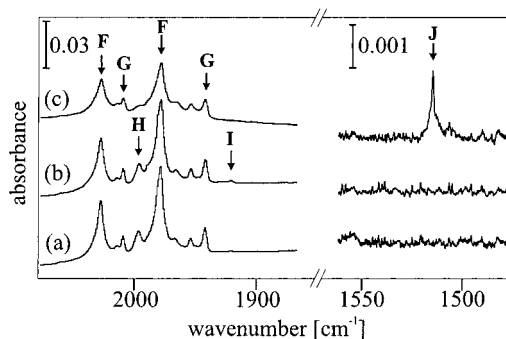


**Figure 7.** IR spectrum of an Ar matrix containing In and 2%  $^{12}\text{CO}$ : (a) following deposition; (b) following UV photolysis ( $\lambda = 200\text{--}400$  nm); and (c) following UV-visible photolysis ( $\lambda = 200\text{--}800$  nm).

matrix splitting. However, some additional, weaker signals at higher frequencies were observed in the spectrum of the Kr matrix, occurring at 2014.6 and 2013.2  $\text{cm}^{-1}$  and at 1932.4, 1929.9, and 1919.5  $\text{cm}^{-1}$ , respectively. Therefore, the possibility that a small proportion of a different molecule is also present cannot be ruled out completely. One possibility is that these features arise from a loosely bound complex between a  $\text{Ga}-(\text{CO})_2$  molecule and an additional Ga atom. Such a complex is observed in our studies of the reaction between indium and carbon monoxide.

**Indium.** Figure 7 depicts the infrared spectra of the matrix formed when gallium was replaced by indium for a CO concentration of 2% in an excess of Ar. Following deposition, the matrix again displayed significant absorptions in the  $\nu(\text{C}-\text{O})$  region supplementing those arising from matrix-isolated carbon monoxide,<sup>34</sup> but now at appreciably higher wavenumbers than in the gallium experiments. Dominating these new features were the two strong bands at 2029.2 and 1980.2  $\text{cm}^{-1}$  which maintained a constant intensity ratio irrespective of the conditions and so could be identified with a single product **F**. These frequencies are within 18  $\text{cm}^{-1}$  of the ones reported earlier and ascribed to  $\text{In}(\text{CO})_2$  by Kasai et al.<sup>22</sup> However, the use of lower concentrations of CO in the present experiments (2% cf. 10%) has provided us with sharper, better defined features. In a series of experiments with argon matrices containing CO at concentrations ranging from 2 to 10%, we have confirmed that increasing the CO concentration does indeed have a highly deleterious effect on bandwidth, thereby impairing the ability of infrared measurements to detect, and discriminate between, different species contained within the matrix (see below). Our studies with matrices containing 2% and less CO have revealed that the bands due to **F** are accompanied by additional features attributable to other indium carbonyls that have been hidden



**TABLE 2: Infrared Absorptions Associated with the Products of the Reactions of In with  $^{12}\text{CO}/(^{12}\text{CO} + ^{13}\text{CO})/^{13}\text{CO}$  (Frequencies in  $\text{cm}^{-1}$ )**

In + $^{12}\text{CO}$	In + $(^{12}\text{CO} + ^{13}\text{CO})$	In + $^{13}\text{CO}$	increase in CO%	$\lambda = 200\text{--}400$ nm photolysis <sup>a</sup>	broad-band photolysis <sup>a</sup>	absorber
2029.2	2029.2	1985.0	↑	↓	↓	In(CO) <sub>2</sub> , <b>F</b>
	2015.4					
	1985.0					
2010.5	2010.5	1966.0	↑	↓	↓	In(CO) <sub>2</sub> ·In, <b>G</b>
	1993.8					
	1966.0					
1996.5	1996.5	1955.4	↓	↓	↓	In·InCO, <b>H</b>
	1955.4					
	1980.2					
1980.2	1980.2	1937.6	↑	↓	↓	In(CO) <sub>2</sub> , <b>F</b>
	1950.0					
	1937.6					
1942.6	1942.6	1900.7	↑	↓	↓	In(CO) <sub>2</sub> ·In, <b>G</b>
	1915.1					
	1900.7					
1920.8	1920.8	1880.5	↓	↓	↓	InCO, <b>I</b>
	1880.5					
	1880.5					
1515.5	1515.5	1482.6	↑	-	↑	In <sup>+</sup> [OCCO] <sup>-</sup> , <b>J</b>
	1513.2					
	1490.0					
	1482.6					
483	<i>b</i>	<i>b</i>	↑	↓	↓	In(CO) <sub>2</sub> , <b>F</b>

<sup>a</sup> ↑: increase in intensity. ↓: decrease in intensity. <sup>b</sup> Intensity too low for detection.

hitherto from experimental observation. Thus, the spectrum was found to include sharp bands at 2010.5, 1996.5, and 1942.6  $\text{cm}^{-1}$  and a very weak feature at 1920.8  $\text{cm}^{-1}$  (see Table 2). Like their more prominent neighbors at higher frequencies, the signals at 2010.5 and 1942.6  $\text{cm}^{-1}$  maintained a constant intensity ratio and are therefore linked to a single but distinct absorber **G**, while the second and the fourth are carried by two different molecules **H** and **I**. The mid-infrared region showed a weak band at 483  $\text{cm}^{-1}$  which probably belonged to the most abundant species **F**. Unfortunately, however, the weakness of the band militated against any test of this assignment, including the detection of any  $^{13}\text{CO}$  counterpart (q.v.).

Photolysis of the matrix with UV light ( $\lambda = 200\text{--}400$  nm) caused the intensities of the infrared bands associated with **F**, **G**, **H**, and **I** to decrease, but did not give rise to any new bands. Photodecomposition of **F**, **G**, **H**, and **I** continued on photolysis with broad-band UV–visible light ( $\lambda = 200\text{--}800$  nm) and still there was no sign of any new feature in the region 2200–1600  $\text{cm}^{-1}$  of the infrared spectrum. Under these conditions, however, the spectrum of the matrix did witness the appearance and growth of a new weak absorption at the unusually low frequency of 1515.5  $\text{cm}^{-1}$  which we associate with a fifth indium-containing complex **J**. Co-condensation studies involving the vapors of group 13 elements and carbon monoxide have provided no precedent for such a product, although similar studies featuring alkali metals and carbon monoxide have revealed, through photolysis of matrix-isolated samples, the formation of products having infrared absorptions at frequencies near 1500  $\text{cm}^{-1}$  and lower.<sup>23,24</sup>

The effects of replacing  $^{12}\text{CO}$  by  $^{13}\text{CO}$  are revealed in the infrared spectra illustrated in Figure 8. The same pattern was observed but the frequency of each of the bands was reduced by 44.5–32.9  $\text{cm}^{-1}$ . It is reasonable therefore to assume that the spectroscopic signatures arise from what are substantially  $\nu(\text{C}\text{--}\text{O})$  fundamentals, if not of indium carbonyls in the conventional sense in each case, of species containing CO oscillators.

Replacement of  $^{12}\text{CO}$  or  $^{13}\text{CO}$  by a mixture of the isotopomers (with  $^{12}\text{CO}:^{13}\text{CO} = \text{ca. } 2:1$ ) yielded an indium-containing matrix with the infrared spectrum shown in Figure 9a. This was

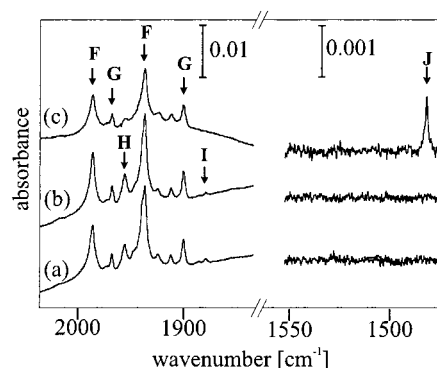


**Figure 8.** IR spectrum of an Ar matrix containing In and 2%  $^{13}\text{CO}$ : (a) following deposition; (b) following UV photolysis ( $\lambda = 200\text{--}400$  nm); and (c) following UV–visible photolysis ( $\lambda = 200\text{--}800$  nm).

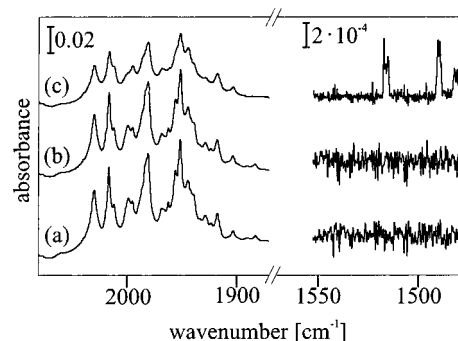


**Figure 9.** IR spectrum of an Ar matrix containing In and a mixture of  $^{12}\text{CO}$  and  $^{13}\text{CO}$  (2:1, total 2%): (a) following deposition; (b) following UV photolysis ( $\lambda = 200\text{--}400$  nm); and (c) following broad-band UV–visible photolysis ( $\lambda = 200\text{--}800$  nm).

characterized by a relative plethora of absorptions in the region 1880–2030  $\text{cm}^{-1}$ . The apparently complicated pattern can be explained on the assumption that each of the two bands associated with the products **F** and **G** is replaced by a *triplet*, implying the presence of two symmetrically equivalent CO groups. On the other hand, **H** and **I** did not give rise to any feature additional to those observed in the experiments with  $^{12}\text{CO}$  and  $^{13}\text{CO}$  taken separately, and appear therefore to be

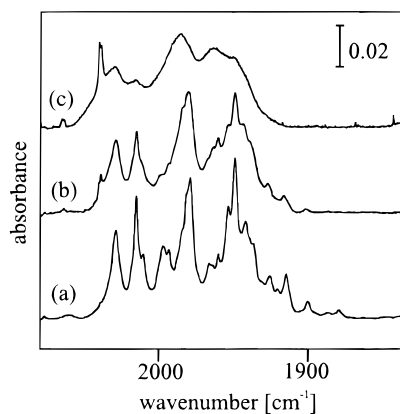


**Figure 10.** IR spectra of Ar matrices containing In and a mixture of  $^{12}\text{CO}$  and  $^{13}\text{CO}$  following deposition: (a) 2% CO; (b) 4.5% CO; and (c) 10% CO.

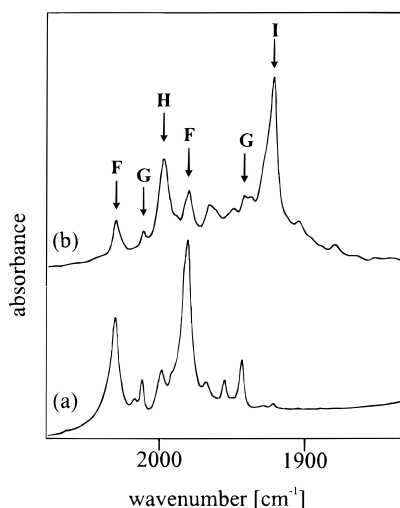


**Figure 11.** IR spectra of Ar matrices containing In and  $^{12}\text{CO}$  at different concentrations: (a) 2% CO; and (b) 0.2% CO.

monocarbonyls. After photolysis with broad-band UV–visible light, the signature of the product **J** was observed to take the form of a highly unsymmetrical *quartet* with components at 1515.5, 1513.2, 1490.0, and 1482.6  $\text{cm}^{-1}$  (see Figure 9c). The remarkably small splittings evidenced for the mixed  $^{12}\text{CO}/^{13}\text{CO}$  species exhibit an unusual decoupling effect manifesting itself through the appearance of one feature that is 2.3  $\text{cm}^{-1}$  red-shifted with respect to the all- $^{12}\text{CO}$  band (1515.5  $\text{cm}^{-1}$ ) and a second that is 7.4  $\text{cm}^{-1}$  blue-shifted with respect to the all- $^{13}\text{CO}$  band (1482.6  $\text{cm}^{-1}$ ). This pattern, allied to the magnitude of the primary  $^{13}\text{C}$  shift, can be understood only in terms of a product containing two *inequivalent* CO oscillators.

As indicated before, CO concentrations of more than 2% resulted in a broadening of the IR signals without the appearance of new ones. As demonstrated in Figure 10, the sharp and distinct absorptions observed for 2% CO concentrations overlap for concentrations of 10% to give a spectrum where only 5 maxima can be spotted. As in the case of Ga, additional experiments were carried out with low concentrations of CO (0.2%). The spectrum obtained after deposition with argon doped with 0.2% CO is shown in Figure 11, together with that for 2% CO concentration. Hence it emerges that the signal due to **I**, which appears to be very weak for 2% CO, dominates the spectrum for 0.2% CO. The signal arising from product **H** also increases in relative intensity. On the other hand, the intensities of the signals at 2029.2, 2010.5, 1980.2, and 1942.6  $\text{cm}^{-1}$  were found to be reduced.

#### 4. Discussion

The main infrared features observed to develop as a result of the reactions between gallium or indium vapors and carbon monoxide occurring through thermal or photolytic activation will be shown to arise from the following compounds: **A**,  $\text{Ga}(\text{CO})_2$ ; **B**,  $\text{Ga}\cdot\text{GaCO}$ ; **C**,  $\text{GaCO}$ ; **D**,  $\text{Ga}(\mu\text{-CO})\text{Ga}$ ; **E**,  $\text{Ga}(\mu\text{-CO})_2\text{Ga}$ ; **F**,  $\text{In}(\text{CO})_2$ ; **G**,  $\text{In}(\text{CO})_2\cdot\text{In}$ ; **H**,  $\text{In}\cdot\text{InCO}$ ; **I**,  $\text{InCO}$ ; and **J**,  $\text{In}^+[\text{OCCO}]^{\cdot-}$ . The assignments will each be justified on the basis of the following criteria: (i) the frequencies of the observed  $\nu(\text{C}-\text{O})$  bands; (ii) the response of the bands to  $^{13}\text{CO}$  enrichment of the relevant absorber; (iii) the response of the bands to alteration of the CO concentration and to alteration of the furnace temperature; (iv) consideration of the properties anticipated by quantum chemical calculations; and (v) comparison with the vibrational properties reported previously for the same or related species.

In carrying out the calculations on the group 13 carbonyls, we considered it essential to use comparable basis sets throughout the series of molecules in order that the *trends* in structures and frequencies should be method-independent. It was also necessary for calculations on the In species to include relativistic corrections. Preliminary comparisons gave satisfactory agreement with experiment using the ADF package with type IV basis sets with small frozen cores for all atoms.<sup>27,28</sup> Details are given in the Experimental Section.

To emphasize the parallels between gallium and indium, we group together the products with the same compositions and structures in the following order: (a)  $\text{Ga}(\text{CO})_2$  and  $\text{In}(\text{CO})_2$ ; (b)  $\text{GaCO}$  and  $\text{InCO}$ ; (c)  $\text{Ga}\cdot\text{GaCO}$  and  $\text{In}\cdot\text{InCO}$ ; (d)  $\text{Ga}(\mu\text{-CO})\text{Ga}$ ; (e)  $\text{In}(\text{CO})_2\cdot\text{In}$ ; (f)  $\text{Ga}(\mu\text{-CO})_2\text{Ga}$ ; and (g)  $\text{In}^+[\text{OCCO}]^{\cdot-}$ .

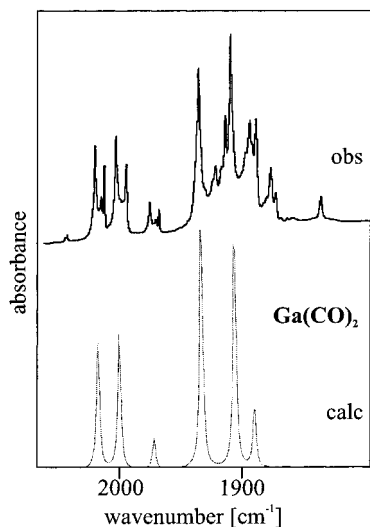
**(a)  $\text{Ga}(\text{CO})_2$  (A) and  $\text{In}(\text{CO})_2$  (F).** On the evidence of their infrared signatures, the products **A** and **F** were the principal products formed in our experiments with gallium and indium vapors, respectively, on co-deposition with CO for CO concentrations of 2% in an excess of argon at 12 K. Each was characterized by two distinct  $\nu(\text{C}-\text{O})$  absorptions which could be detected at the lowest metal concentrations employed, and is likely therefore to contain only a single metal atom. That it represented the ultimate product of the thermal reaction between the atoms in their ground electronic state and an excess of CO was indicated by the growth of the bands in annealing experiments when the matrix was allowed to warm to ca. 30 K so as to encourage diffusion.

In the case of **A** the absorptions occurred at 2016.8 and 1933.6  $\text{cm}^{-1}$  but were each split into a triplet, presumably through the occupancy of different matrix sites by the molecule. Similar multiplet patterns have been reported for the analogous bands of  $\text{Al}(\text{CO})_2$  under comparable conditions.<sup>12</sup> The experiment with a 2:1 mixture of  $^{12}\text{CO}$  and  $^{13}\text{CO}$  then gave good grounds for believing that **A** is the gallium analogue of  $\text{Al}(\text{CO})_2$ , in keeping with the conclusions drawn from earlier studies.<sup>13,19,20</sup> The appearance of just two prominent signals in the experiments carried out with krypton matrices (2006.1 and 1909.3  $\text{cm}^{-1}$ ) supports the view that the triplet structure is a consequence of matrix splitting. However, weak, neighboring absorptions in the spectrum of the Kr matrix leave open the possibility that a slightly different species, e.g.  $\text{Ga}(\text{CO})_2\cdot\text{Ga}$ , is also present. With reference to the strongest component in each set of triplet absorptions, the intensity ratio  $I_{1933.6}/I_{2016.8}$  was observed to be 1.92:1. If it is assumed that the antisymmetric  $\nu(\text{C}-\text{O})$  mode occurs at lower frequency than the symmetric one (as is normally the case in dicarbonyl molecules), and that the CO dipole moment derivatives are directed along the CO bonds, this implies that the CO groups subtend an angle  $\theta$  of about

**TABLE 3: Observed and Calculated Frequencies (in  $\text{cm}^{-1}$ ) for (a)  $\text{Ga}(\text{CO})_2$  and (b)  $\text{In}(\text{CO})_2$** 

obsd	calcd <sup>a</sup>	assignment
(a) $\text{Ga}(\text{CO})_2$		
1933.6	1933.6	$\nu_{\text{asym}}[\text{Ga}(\text{CO})_2]$
1907.8	1906.5	$\nu_{\text{asym}}[\text{Ga}(\text{CO})(\text{CO})]$
1892.9	1890.5	$\nu_{\text{asym}}[\text{Ga}(\text{CO})_2]$
2016.8	2016.8	$\nu_{\text{sym}}[\text{Ga}(\text{CO})_2]$
1999.4	1999.8	$\nu_{\text{sym}}[\text{Ga}(\text{CO})(\text{CO})]$
1972.8	1971.8	$\nu_{\text{sym}}[\text{Ga}(\text{CO})_2]$
(b) $\text{In}(\text{CO})_2$		
1980.2	1980.8	$\nu_{\text{asym}}[\text{In}(\text{CO})_2]$
1949.7	1950.0	$\nu_{\text{asym}}[\text{In}(\text{CO})(\text{CO})]$
1937.6	1936.7	$\nu_{\text{asym}}[\text{In}(\text{CO})_2]$
2029.2	2029.6	$\nu_{\text{sym}}[\text{In}(\text{CO})_2]$
2015.4	2015.7	$\nu_{\text{sym}}[\text{In}(\text{CO})(\text{CO})]$
1985.0	1984.3	$\nu_{\text{sym}}[\text{In}(\text{CO})_2]$

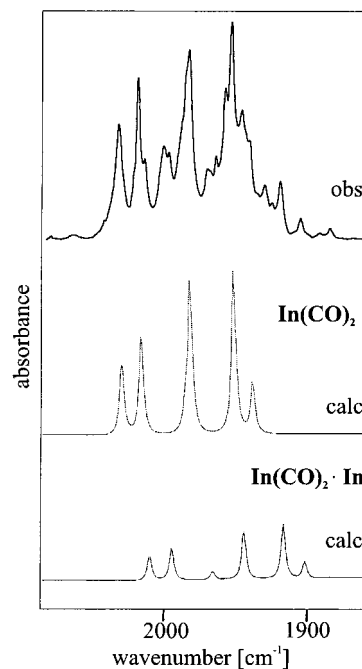
<sup>a</sup> Simulation on the basis of a frequency-factored force field.



**Figure 12.** Comparison of the IR spectrum measured for  $\text{Ga}(\text{CO})_2$  isolated in an Ar matrix and prepared from a mixture of  $^{12}\text{CO}$  and  $^{13}\text{CO}$  (2:1, total 2%) with the spectrum simulated on the basis of a frequency-factored force field.

$108^\circ$ . We have sought to simulate the  $\nu(\text{C}-\text{O})$  region of the infrared spectrum when the molecule is partially enriched in  $^{13}\text{CO}$  on the basis of an energy-factored force field. The optimum fit to the observed spectrum was achieved with  $\theta = 110^\circ$  and the force constants  $k_{\text{CO}} = 1577 \text{ N m}^{-1}$  and  $k_{\text{CO,CO}} = 66 \text{ N m}^{-1}$  (see Table 3a and Figure 12). For  $\text{Ga}(\text{CO})_2$ , then, we believe that  $\theta$  comes close to the value of  $110^\circ \pm 5^\circ$  estimated by similar methods for  $\text{Al}(\text{CO})_2$ ,<sup>10,12</sup> while falling short of the earlier estimate of  $120^\circ \pm 5^\circ$ .<sup>13,19</sup>

**F** was characterized by two prominent  $\nu(\text{C}-\text{O})$  absorptions centered at 2029.2 and 1980.2  $\text{cm}^{-1}$ . Scrutiny of the spectrum of **F** when partially enriched in  $^{13}\text{CO}$ , with due allowance for the proximity of the corresponding features of **G**, indicates that each of these bands gives place to a triplet pattern (one component being discernible only as a shoulder on the flank of the intense absorption near 1980  $\text{cm}^{-1}$ ). As with the product signals assigned to  $\text{Ga}(\text{CO})_2$ , **A**, a small increase in intensity was observed for the bands due to **F** in the annealing experiments. Hence there is every reason to believe that **F** is  $\text{In}(\text{CO})_2$  with two equivalent CO groups completing an angular structure akin to that of  $\text{Ga}(\text{CO})_2$  with  $C_{2v}$  symmetry. This assignment is consistent with earlier studies in which larger concentrations of CO (10%) were used.<sup>22</sup> The spectrum reported previously resembles the spectrum shown here for 10% CO concentration

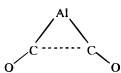
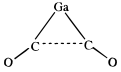
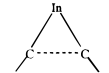


**Figure 13.** Comparison of the IR spectra measured for  $\text{In}(\text{CO})_2$  and  $\text{In}(\text{CO})_2 \cdot \text{In}$  isolated in an Ar matrix and prepared from a mixture of  $^{12}\text{CO}$  and  $^{13}\text{CO}$  (2:1, total 2%) with the spectra simulated on the basis of frequency-factored force fields.

(see Figure 10). The large half-widths of the signals at this high concentration prevented the detection of products other than the dicarbonyl in the previous study. The relative intensities of the two  $\nu(\text{C}-\text{O})$  bands due to the all- $^{12}\text{CO}$  isotopomer,  $I_{1980.2}/I_{2029.2} = 1.69:1$ , indicate that  $\theta$  is about  $105^\circ$  in this case. Simulation of the spectrum associated with the molecule on partial enrichment in  $^{13}\text{CO}$  gives the optimum fit illustrated in Figure 13 and detailed in Table 3b on the basis of  $\theta = 105^\circ$  and of the force constants  $k_{\text{CO}} = 1625 \text{ N m}^{-1}$  and  $k_{\text{CO,CO}} = 39 \text{ N m}^{-1}$ . It appears therefore that the CO bonds are somewhat stronger—and the metal–carbon bonds presumably weaker—in  $\text{In}(\text{CO})_2$  than in  $\text{Ga}(\text{CO})_2$ : moreover, the CO groups subtend a marginally tighter angle in the indium compound. It is possible that the weak absorption at 483  $\text{cm}^{-1}$  represents a fundamental involving a significant degree of In–C stretching. In that case, there would be an obvious analogy with  $\text{Al}(\text{CO})_2$  for which a band at 497.0  $\text{cm}^{-1}$  has been sighted and assigned to a hybrid motion which is part  $\nu(\text{Al}-\text{C})$  and part  $\delta(\text{Al}-\text{C}-\text{O})$ . A frequency lower than 483  $\text{cm}^{-1}$  might then have been expected for  $\text{In}(\text{CO})_2$ , but changes in the makeup of the vibration could well result in only a modest change of frequency. Without more information about the band at 483  $\text{cm}^{-1}$ , however, any assignment must be a matter of speculation.

For additional information about the properties of  $\text{Ga}(\text{CO})_2$  and  $\text{In}(\text{CO})_2$  we have drawn on the results of various DFT calculations. Table 4 give a summary of the results obtained for  $\text{Al}(\text{CO})_2$ ,  $\text{Ga}(\text{CO})_2$ , and  $\text{In}(\text{CO})_2$ . The optimum structure deduced in this way for  $\text{Ga}(\text{CO})_2$  resembles closely that deduced previously for  $\text{Al}(\text{CO})_2$ <sup>14</sup> with  $\angle\text{C}-\text{Ga}-\text{C} = 72.6^\circ$  and  $\text{Ga}-\text{C}-\text{O}$  arms bent slightly outward so that  $\angle\text{Ga}-\text{C}-\text{O} = 163.1^\circ$ . This implies that the CO groups subtend an angle  $\theta = 106.4^\circ$  to each other, in pleasing agreement with the results of our experiments. The minimum-energy geometry of  $\text{In}(\text{CO})_2$  follows the precedents set by the lighter congeners. It features an even tighter  $\text{C}-\text{M}-\text{C}$  angle ( $61.9^\circ$ ) and  $\text{M}-\text{C}-\text{O}$  arms again bent slightly outward so that  $\angle\text{M}-\text{C}-\text{O} = 174.0^\circ$ . It implies that  $\theta$  is  $74^\circ$ , i.e., considerably smaller than the experimental estimate,

**TABLE 4: Geometries and  $\nu(\text{C}-\text{O})$  Frequencies Calculated Using DFT Methods for  $\text{M}(\text{CO})_2$  Molecules ( $\text{M} = \text{Al}, \text{Ga}, \text{or In}$ )**

compound	$S$	symmetry	structure	energy [kJ mol <sup>-1</sup> ] <sup>a</sup>	$\nu(\text{C}-\text{O})$ [cm <sup>-1</sup> ]	obs. $\nu(\text{C}-\text{O})$ [cm <sup>-1</sup> ]	
$\text{Al}(\text{CO})_2$	$\frac{1}{2}$	$C_{2v}$		Al-C: 2.044 Å, C-O: 1.162 Å, C-Al-C: 73.5°, Al-C-O: 165.4°	-176	1953	1995.3 <sup>b</sup>
						1905	1988.7 <sup>b</sup>
$\text{Ga}(\text{CO})_2$	$\frac{1}{2}$	$C_{2v}$		Ga-C: 2.169 Å, C-O: 1.158 Å, C-Ga-C: 72.6°, Ga-C-O: 163.1°	-125	1972	2016.8
						1911	2011.8
							1912.4
$\text{In}(\text{CO})_2$	$\frac{1}{2}$	$C_{2v}$		In-C: 2.561 Å, C-O: 1.155 Å, C-In-C: 61.8°, In-C-O: 174.0°	-85	1971	1933.6
						1909	1920.4
							1912.4
							2029.2
							1985.0

<sup>a</sup> Energy given with respect to M in <sup>3</sup>P state and CO. <sup>b</sup> Reference 12.

while appearing correctly to anticipate that the angle decreases with the switch from  $\text{Ga}(\text{CO})_2$  to  $\text{In}(\text{CO})_2$ . The calculations conform with experimental findings here and elsewhere<sup>12</sup> to the effect that the CO bonds become shorter in the order  $\text{Al}(\text{CO})_2 > \text{Ga}(\text{CO})_2 > \text{In}(\text{CO})_2$ , suggesting that the strength of the M-C interaction follows the *reverse* order.

A feature at odds with the structures normally found for metal carbonyls<sup>1-4</sup> is the nonlinear nature of the M-C-O units. This may reflect simply the achievement of optimum overlap between the vacant np valence orbital of M coincident with the 2-fold axis of the molecule and the  $n, \pi$  orbitals of the CO ligands. By contrast, the  $\pi$ -type bonding resulting from the overlap of orbitals perpendicular to the molecular plane is not affected greatly by small changes in the M-C-O geometry. Alternative explanations of the nonlinearity of these units include (i) repulsive interaction between the metal  $ns^2$  electrons and the  $5\sigma$  donor pair on CO (by analogy with the bending predicted to occur in MCO molecules formed by the group 13 elements<sup>16</sup>), (ii) the establishment of a C...C interaction between the two CO groups admissible to the bonding scheme, say, through an O=C=C=O contribution to the ground-state wave function;<sup>12</sup> or (iii) Coulombic repulsion between the O atoms which carry a small but significant negative charge and are otherwise brought unusually close together by the narrow C-M-C angle. We have no means of assessing the importance of the various factors and indeed doubt the ability of current, standard theoretical methods accurately and consistently to model this feature for a wide range of group 13 elements.

The electronic structure calculations give an outer configuration for  $\text{In}(\text{CO})_2$  of  $\dots b_2^2 a_1^2 b_1^1$  (the molecule lying in the  $xz$  plane). Iso-surfaces and energies for these orbitals are shown in Figure 14. The half-occupied  $b_1$  orbital is In-C  $\pi$  bonding and also C-C  $\pi$  bonding. The  $a_1$  HOMO has In  $\sigma$  lone pair character and the  $b_2$  HOMO-1 is C-C antibonding. Excitation of an electron into the  $b_1$  orbital should increase the bonding between the two C atoms. When the geometry of  $\text{In}(\text{CO})_2$  was optimized with  $C_{2v}$  symmetry and a  $\dots b_2^2 a_1^1 b_1^2$  configuration, the C-C distance shortened to 1.423 Å. This excited state lay 2.20 eV above the ground state. The increased C-C interaction on excitation supports the suggestion that  $\text{In}(\text{CO})_2$  is the precursor to the species **J**, which will be identified as the charge-transfer complex  $\text{In}^+[\text{OCCO}]^-$ .

(b) **GaCO (C) and InCO (I, C and I)** were each characterized by a  $\nu(\text{C}-\text{O})$  band which was invariably weak for CO

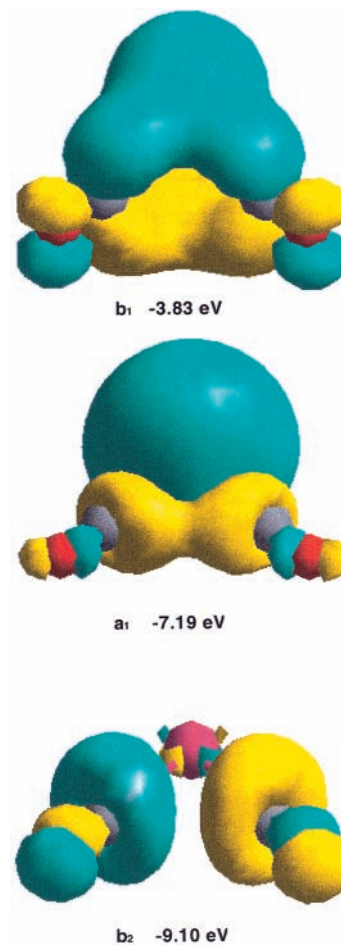


**Figure 14.** Iso-surfaces and energies for the outer configuration ( $\dots b_2^2 a_1^2 b_1^1$ ) of  $\text{In}(\text{CO})_2$ .

concentrations of 2% but which dominated the spectra obtained for low CO concentrations (0.2%). In their isotopically natural forms **C** and **I** could be identified by absorptions at 1875.6/1866.5 and 1920.8 cm<sup>-1</sup>, respectively. With <sup>13</sup>CO alone these shifted to 1834.6/1825.9 and 1880.5 cm<sup>-1</sup>, and no additional absorption was seen in experiments involving a mixture of <sup>12</sup>CO and <sup>13</sup>CO. The intensities of the relevant bands decreased on UV photolysis of the matrix and decreased again when the range of photolyzing wavelengths was extended to include the visible



**TABLE 5: Geometries and  $\nu(\text{C}-\text{O})$  Frequencies of Group 13 Metal Monocarbonyls Calculated Using DFT Methods<sup>a</sup>**

molecule	2S + 1	calculated, this work				calculated, ref 16 <sup>b</sup>				obsd $\nu(\text{C}-\text{O})$	energy <sup>c</sup>
		$r_e(\text{M}-\text{C})$	$r_e(\text{C}-\text{O})$	$\angle\text{M}-\text{C}-\text{O}$	$\nu(\text{C}-\text{O})$	$r_e(\text{M}-\text{C})$	$r_e(\text{C}-\text{O})$	$\angle\text{M}-\text{C}-\text{O}$	$\nu(\text{C}-\text{O})$		
BCO	4					1.426 (1.433)	1.179 (1.189)	180	2059 (1997)	2002.3 <sup>c</sup>	
AlCO	2	2.146	1.167	168.3	1890	2.088 (2.132)	1.169 (1.176)	170 (173)	1942 (1889)	1867.7 <sup>d</sup>	-81
	4					1.847 (1.865)	1.181 (1.189)	180	1911 (1853)		
GaCO	2	2.254	1.164	180	1898	2.150 (2.226)	1.166 (1.173)	180	1954 (1891)	1875.6	-61
	4					1.816 (1.845)	1.184 (1.193)	180	1905 (1838)		
InCO	2	2.582	1.159	180	1909	2.377 (2.440)	1.164 (1.172)	180	1962 (1896)	1920.8	-43
	4					2.039 (2.074)	1.179 (1.187)	180	1909 (1841)		

<sup>a</sup> Bond distances in Å, bond angles in deg, frequencies in  $\text{cm}^{-1}$ , and energies in  $\text{kJ mol}^{-1}$ . <sup>b</sup> First value based on local spin-density approximation; value in parentheses allows for exchange and correlation. <sup>c</sup> Reference 18. <sup>d</sup> Reference 12. <sup>e</sup> Energy given with respect to M in  $^2\text{P}$  state and CO.

region ( $200 < \lambda < 800$  nm). Both product signals were found to grow slightly when the matrix was annealed, presumably as a result of reactions between uncoordinated Ga or In atoms and CO. The circumstances clearly suggest that **C** is GaCO occupying two different matrix sites and that **I** is InCO. Given that  $\nu(\text{C}-\text{O}) = 1867.7$   $\text{cm}^{-1}$  for AlCO under similar conditions,<sup>12</sup> the present results reveal a steady increase in frequency in the series AlCO < GaCO < InCO for the molecule in the most populated site (site I for GaCO) from which we infer a steady *decrease* in the M–C bond strength. As expected,  $\nu(\text{C}-\text{O})$  for MCO occurs at a frequency (in  $\text{cm}^{-1}$ ) appreciably lower than the mean of the corresponding frequencies for  $\text{M}(\text{CO})_2$  (cf. AlCO 1867.7,  $\text{Al}(\text{CO})_2$  1951.5; GaCO 1875.6,  $\text{Ga}(\text{CO})_2$  1975.2; InCO 1920.8,  $\text{In}(\text{CO})_2$  2004.7). This feature emphasizes the competition that is introduced by coordination of a second CO molecule in the  $\text{M}(\text{CO})_2$  species. The results are also difficult to reconcile with the findings of an earlier theoretical study giving us to believe that AlCO is much less strongly bound than is  $\text{Al}(\text{CO})_2$  (the estimated total binding energies being 17–20 and 71  $\text{kJ mol}^{-1}$ , respectively).<sup>14</sup>

The properties of the group 13 monocarbonyls have been investigated previously using local density-functional calculations within the framework of linear combinations of Gaussian-type orbitals.<sup>16</sup> BCO probably assumes a linear  $^4\Sigma^+$  ground electronic state,<sup>16,17</sup> whereas the remaining monocarbonyls are more likely to be spin doublets, leaving open the question of whether the linear  $^2\Pi$  state is unstable to bending. Table 5 presents the dimensions and  $\nu(\text{C}-\text{O})$  frequencies we have calculated for these MCO molecules with the aid of the Amsterdam Density Functional program system. Spin-orbit effects have not been included, although these may well have an important influence on the geometries of monocarbonyls of the heavier group 13 elements. The table also includes for comparison the results of the earlier calculations,<sup>16</sup> as well as the experimental  $\nu(\text{C}-\text{O})$  frequencies. The two sets of calculations give results in close agreement and the  $\nu(\text{C}-\text{O})$  frequencies reflect well the observed trend in the series AlCO, GaCO, and InCO, even if they both underestimate the spread of these frequencies. The earlier calculations<sup>16</sup> also reproduce pleasingly well the decrease in M–CO bond strength implied by the measured  $\nu(\text{C}-\text{O})$  frequencies (with estimated M–CO bond dissociation energies of 93, 80, and 73  $\text{kJ mol}^{-1}$  for M = Al, Ga, and In, respectively, very different from those first attributed<sup>14</sup> to molecules of this type). The trend reflects decreased  $\sigma$ -donation and  $\pi$ -back-donation as the atomic number of M increases, presumably because of the increasing M–C distances and decreasing orbital-energy match and overlap. The point has also been made previously<sup>16</sup> that the group 13 monocarbonyls are unlike transition-metal carbonyls in that they afford no obvious correlation between  $\nu(\text{C}-\text{O})$  and the extent of  $\pi$ -back-donation.

The earlier theoretical analysis<sup>16</sup> has shown, furthermore, that excitation of the metal atoms into the  $^4\text{P}$  state (electron configuration  $ns^1np^2$ ), where the repulsion is much less, gives a linear MCO adduct with a much stronger and shorter M–C bond. The resulting  $^4\Sigma^+$  state of the molecule has been shown to be unstable with respect to dissociation to M in its ground electronic state and CO. Excitation to this state, despite its dependence on a spin-forbidden transition, may then account for the decomposition of both GaCO and InCO upon photolysis.

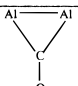
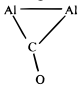
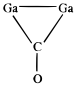
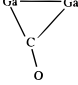
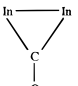
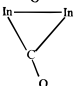
**(c) Ga·GaCO (B) and In·InCO (H).** Unlike the bands associated with  $\text{Ga}(\text{CO})_2$ , the single feature assigned to **B** gives rise to a doublet when the matrix contains a mixture of  $^{12}\text{CO}$  and  $^{13}\text{CO}$  with components at 1898.1 and 1857.8  $\text{cm}^{-1}$  corresponding to the all- $^{12}\text{CO}$  and all- $^{13}\text{CO}$  isotopomers, respectively. Moreover, the formation of this product was shown to be favored by reducing the CO concentration. The obvious inference is that **B** has the composition  $\text{Ga}_2\text{CO}$ . **B** has a  $\nu(\text{C}-\text{O})$  mode at slightly higher frequency than does GaCO (1898.1 vs 1875.6  $\text{cm}^{-1}$ ) implying a marginal weakening of the Ga–CO bond through the attachment of the second Ga atom. A signal at the same position as the one we observe for  $\text{Ga}_2\text{CO}$  has previously been assigned to GaCO.<sup>13</sup> On the grounds of the experiments carried out for different CO concentrations (see Figure 5) and furnace temperatures, however, the doublet at 1875.6/1866.5  $\text{cm}^{-1}$  has to be assigned to GaCO.

The doublet pattern found in the experiments with a mixture of  $^{12}\text{CO}$  and  $^{13}\text{CO}$ , with frequencies at the same positions as the ones observed in the experiments with  $^{12}\text{CO}$  and  $^{13}\text{CO}$  alone (1996.5 and 1955.4  $\text{cm}^{-1}$ , respectively), indicates that **H**, like **B**, contains only one CO group. Because of the similar response of the signals associated with **H** and **B** to changes in the CO concentration or furnace temperature, **H** can be identified with a species having the composition  $\text{In}_2\text{CO}$ . As with  $\text{Ga}_2\text{CO}$ , the  $\nu(\text{C}-\text{O})$  frequency of  $\text{In}_2\text{CO}$  is blue-shifted with respect to the corresponding frequency of InCO (1920.8  $\text{cm}^{-1}$ ), indicating that the second In atom leads to a slightly stronger C–O bond.

DFT calculations were unable, however, to find a potential energy minimum for the structure of either  $\text{Ga}_2\text{CO}$  or  $\text{In}_2\text{CO}$  that retained a terminal CO group. The most likely interpretation therefore is that the two metal atoms are not bound together but that the species are contact pairs most aptly formulated as  $\text{M}\cdot\text{MCO}$  (M = Ga or In).

**(d) Ga( $\mu$ -CO)Ga (D).** The signal at 1828.0  $\text{cm}^{-1}$ , attributed to the species **D**, was found to increase with lower CO concentrations and thus it belongs to a species containing only one CO group. For aluminum in analogous circumstances a  $\nu(\text{C}-\text{O})$  signal at 1737.1  $\text{cm}^{-1}$  has been assigned to the bridged species  $\text{Al}(\mu\text{-CO})\text{Al}$ .<sup>12</sup> The species **D** is most likely to be the Ga analogue  $\text{Ga}(\mu\text{-CO})\text{Ga}$ . The red shifts of 70.1 and 47.6  $\text{cm}^{-1}$  compared with the  $\nu(\text{C}-\text{O})$  modes of  $\text{Ga}_2\text{CO}$  and GaCO, respectively, indicate a weakening of the CO bond, as expected

**TABLE 6: Geometries and  $\nu(\text{C-O})$  Frequencies of Monobridged  $\text{M}(\mu\text{-CO})\text{M}$  Species ( $\text{M} = \text{Al}, \text{Ga},$  or  $\text{In}$ ) Calculated Using DFT Methods**

compound	$S$	symmetry	structure	energy [kJ mol <sup>-1</sup> ] <sup>a</sup>	$\nu(\text{C-O})$ [cm <sup>-1</sup> ]	obs. $\nu(\text{C-O})$ [cm <sup>-1</sup> ]
$\text{Al}(\mu\text{-CO})\text{Al}$	0	$C_{2v}$		Al-Al: 2.445 Å, Al-C: 2.108 Å, C-O: 1.190 Å, Al-C-Al: 70.9°	-271	1741
$\text{Al}(\mu\text{-CO})\text{Al}$	1	$C_s$		Al(1)-Al(2): 2.645 Å, Al(1)-C: 2.042 Å, Al(2)-C: 2.440 Å, C- O: 1.162 Å, Al-C-Al: 71.7°, Al- C-O: 166.4°	-279	1766
$\text{Ga}(\mu\text{-CO})\text{Ga}$	0	$C_{2v}$		Ga-Ga: 2.423 Å, Ga-C: 2.170 Å, C-O: 1.180 Å, Ga-C-Ga: 67.6°	-220	1798
$\text{Ga}(\mu\text{-CO})\text{Ga}$	1	$C_s$		Ga(1)-Ga(2): 2.659 Å, Ga(1)-C: 2.132 Å, Ga(2)-C: 2.562 Å, C- O: 1.173 Å, Ga-C-Ga: 68.3°, Ga-C-O: 169.2°	-230	1815
$\text{In}(\mu\text{-CO})\text{In}$	0	$C_{2v}$		In-In: 2.802 Å, In-C: 2.484 Å, C-O: 1.172 Å, In-C-In: 68.7°	-159	1832
$\text{In}(\mu\text{-CO})\text{In}$	1	$C_s$		In(1)-In(2): 3.084 Å, In(1)-C: 2.471 Å, In(2)-C: 2.868 Å, C-O: 1.167 Å, In-C-In: 70.1°, In-C- O: 173.2°	-188	1839

<sup>a</sup> Energy given with respect to M in <sup>2</sup>P state and CO. <sup>b</sup> Reference 12.

**TABLE 7: Observed and Calculated Frequencies (in cm<sup>-1</sup>) for  $\text{In}(\text{CO})_2\cdot\text{In}$** 

obsd	calcd <sup>a</sup>	assignment
1942.6	1943.3	$\nu_{\text{asym}}[\text{In}(\text{CO})_2\cdot\text{In}]$
1915.1	1915.0	$\nu_{\text{asym}}[\text{In}(\text{CO})(\text{CO})\cdot\text{In}]$
1900.7	1900.0	$\nu_{\text{asym}}[\text{In}(\text{CO})_2\cdot\text{In}]$
2010.5	2010.5	$\nu_{\text{sym}}[\text{In}(\text{CO})_2\cdot\text{In}]$
1993.8	1994.7	$\nu_{\text{sym}}[\text{In}(\text{CO})(\text{CO})\cdot\text{In}]$
1966.0	1965.7	$\nu_{\text{sym}}[\text{In}(\text{CO})_2\cdot\text{In}]$

<sup>a</sup> Simulation on the basis of a frequency-factored force field.

for a bridged structure. The calculated frequency of 1815 cm<sup>-1</sup> (in the case of  $S = 1$ , see Table 6) is in good agreement with the experimental value. The calculated Ga...Ga distance of 2.659 Å suggests bonding between the Ga atoms. The species **D** is almost completely destroyed by photolysis with light having  $\lambda = 200\text{--}400$  nm. At the same time the signal at 1774 cm<sup>-1</sup> belonging to the species **E** appears, suggesting that **D** is the precursor to **E**. We will see that the structures of both molecules are related, with **E** having only an extra bridging CO group.

(e)  $\text{In}(\text{CO})_2\cdot\text{In}$  (**G**). **G** features two  $\nu(\text{C-O})$  bands, namely at 2010.5 and 1942.3 cm<sup>-1</sup>, each of which is split into a triplet when <sup>12</sup>CO is replaced by a mixture of <sup>12</sup>CO and <sup>13</sup>CO. This behavior, allied to the relatively high  $\nu(\text{C-O})$  frequencies, implies that **G** is a molecule with two equivalent terminal CO groups attached to the same or different metal atoms. The observed  $\nu(\text{C-O})$  spectrum can be successfully simulated on the assumption that the CO groups subtend an angle  $\theta = 109^\circ$  and that  $k_{\text{CO}} = 1579$  N m<sup>-1</sup> and  $k_{\text{CO,CO}} = 54$  N m<sup>-1</sup> (see Table 7). The magnitude of these parameters, and particularly of  $\theta$  and the interaction force constant, favors strongly a molecule with both the CO groups bound to the same In atom. Coordination of what is then  $\text{In}(\text{CO})_2$  by a second In atom is seen therefore to result in a significant reduction in the  $\nu(\text{C-O})$  frequencies (and  $k_{\text{CO}}$  force constant) to values not far removed from those of  $\text{Ga}(\text{CO})_2$ . Hence it appears that the In-CO bond is strengthened by the presence of the second In atom. DFT calculations failed to identify a potential energy minimum with any species having the composition  $\text{In}_2(\text{CO})_2$  that was consistent with the properties ascribed to **G** by its IR spectrum. Accord-

**TABLE 8: Observed and Calculated Frequencies (in cm<sup>-1</sup>) for  $\text{Ga}(\mu\text{-CO})_2\text{Ga}$** 

obsd	calcd <sup>a</sup>	assignment
1774.0	1775.2	$b_{2u}[\text{Ga}(\mu\text{-CO})(\mu\text{-CO})\text{Ga}]$
1752.8	1753.7	$a_1[\text{Ga}(\mu\text{-CO})(\mu\text{-CO})\text{Ga}]$
1736.8	1735.6	$b_{2u}[\text{Ga}(\mu\text{-CO})(\mu\text{-CO})\text{Ga}]$
<i>b</i>	2038.7	$a_g[\text{Ga}(\mu\text{-CO})(\mu\text{-CO})\text{Ga}]$
<i>c</i>	2017.7	$a_1[\text{Ga}(\mu\text{-CO})(\mu\text{-CO})\text{Ga}]$
<i>b</i>	1993.2	$a_g[\text{Ga}(\mu\text{-CO})(\mu\text{-CO})\text{Ga}]$

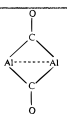
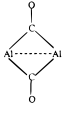
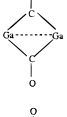
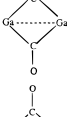
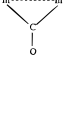
<sup>a</sup> Simulation on the basis of a frequency-factored force field. <sup>b</sup> Infrared-inactive modes. <sup>c</sup> Too weak to be observed.

ingly we are led to the conclusion that **G** is a loosely bound adduct best formulated as  $\text{In}(\text{CO})_2\cdot\text{In}$ .

(f)  $\text{Ga}(\mu\text{-CO})_2\text{Ga}$  (**E**). **E** is derived from one or both of the products **A** and **D** and/or Ga atoms or aggregates also present in the matrix under the action of UV photolysis; it is photolabile under visible light. Its infrared signature is a  $\nu(\text{C-O})$  band at unusually low frequency for a gallium carbonyl, viz., 1774.0 cm<sup>-1</sup>, and which is replaced by a triplet in experiments with a mixture of <sup>12</sup>CO and <sup>13</sup>CO. The formation of **E** was also found to be favored by relatively metal-rich matrix conditions. All the signs are consistent with a digallium carbonyl  $\text{Ga}_2(\text{CO})_2$  incorporating two equivalent CO groups. Previous studies of aluminum<sup>12</sup> and gallium<sup>13</sup> carbonyls afford no direct precedent for such a species. The low frequency of the  $\nu(\text{C-O})$  mode suggests parallels with the dialuminum species  $\text{Al}(\mu\text{-CO})\text{Al}$  (1737.1 cm<sup>-1</sup>) and  $\text{OAl}(\mu\text{-CO})_2\text{AlCO}$  (1881.8 and 1717.1 cm<sup>-1</sup>).<sup>12</sup> Unlike the first of these, however, **E** contains more than one CO group, and unlike the second it does not apparently contain terminal CO groups. The only obvious conclusion, consistent with all the facts available, is that **E** is  $\text{Ga}(\mu\text{-CO})_2\text{Ga}$  with the structure illustrated in Figure 4. We can simulate the observed triplet pattern associated with all the possible <sup>12</sup>CO/<sup>13</sup>CO isotopomers on the assumption that the bridging CO groups are collinear (i.e.,  $\theta = 180^\circ$ ) and with the force constants  $k_{\text{CO}} = 1476$  N m<sup>-1</sup> and  $k_{\text{CO,CO}} = 203$  N m<sup>-1</sup> (see Table 8).

Further information about the likely properties of this new gallium carbonyl has been sought from DFT calculations (see Table 9). We find a singlet minimum-energy planar structure with  $D_{2h}$  symmetry identical with that suggested by the

**TABLE 9: Geometries and  $\nu(\text{C}-\text{O})$  Frequencies of Dibrigged  $\text{M}(\mu\text{-CO})_2\text{M}$  Species ( $\text{M} = \text{Al}, \text{Ga}, \text{or In}$ ) As Calculated Using DFT Methods**

compound	<i>S</i>	symmetry	structure	energy [kJ mol <sup>-1</sup> ] <sup>a</sup>	$\nu(\text{C}-\text{O})$ [cm <sup>-1</sup> ]	$\nu(\text{C}-\text{O})$ obs. [cm <sup>-1</sup> ]	
$\text{Al}(\mu\text{-CO})_2\text{Al}$	0	$D_{2h}$		Al-Al 3.073 Å, Al-C 2.097 Å, C-O 1.186 Å, Al-C-Al: 94.2°	-343	1799 ( $a_{1g}$ ) 1738 ( $b_{2u}$ )	
$\text{Al}(\mu\text{-CO})_2\text{Al}$	1	$D_{2h}$		Al-Al 3.151 Å, Al-C 2.152 Å, C-O 1.193 Å, Al-C-Al: 94.1°	-352	1765 ( $a_{1g}$ ) 1665 ( $b_{2u}$ )	
$\text{Ga}(\mu\text{-CO})_2\text{Ga}$	0	$D_{2h}$		Ga-Ga 3.188 Å, Ga-C 2.155 Å, C-O 1.178 Å, Ga-C-Ga: 95.4°	-265	1836 ( $a_{1g}$ ) 1773 ( $b_{2u}$ )	1774
$\text{Ga}(\mu\text{-CO})_2\text{Ga}$	1	$D_{2h}$		Ga-Ga 3.251 Å, Ga-C 2.226 Å, C-O 1.184 Å, Ga-C-Ga: 93.8°	-292	1811 ( $a_{1g}$ ) 1708 ( $b_{2u}$ )	
$\text{In}(\mu\text{-CO})_2\text{In}$	1	$D_{2h}$		In-In 3.761 Å, In-C 2.521 Å, C-O 1.178 Å, In-C-In: 96.5°	-219	1820 ( $a_{1g}$ ) 1739 ( $b_{2u}$ )	

<sup>a</sup> Energy given with respect to M in <sup>2</sup>P state and CO.

experimental results, with the following dimensions (distances in Å, angles in deg): Ga···Ga 3.188; Ga-C 2.155; C-O 1.178;  $\angle\text{Ga}-\text{C}-\text{Ga}$  95.4°. The relatively long Ga···Ga distance (cf. 2.4–2.6 Å in systems where there is direct Ga–Ga bonding<sup>35</sup>) implies that the Ga–Ga bond has effectively been ruptured in  $\text{Ga}(\mu\text{-CO})_2\text{Ga}$ . The calculated frequency (1773 cm<sup>-1</sup> for the B<sub>2u</sub> mode for the molecule in the singlet state) is in excellent agreement with the observed one (1774 cm<sup>-1</sup>). The calculations offer little prospect of detecting any other infrared bands due to  $\text{Ga}(\mu\text{-CO})_2\text{Ga}$  [the second most intense band having a calculated intensity less than 4% of that associated with the out-of-phase  $\nu(\text{C}-\text{O})$  mode].

On the evidence of our experiments, the digallium monocarbonyl  $\text{Ga}(\mu\text{-CO})\text{Ga}$  (**D**) is the most likely precursor to  $\text{Ga}(\mu\text{-CO})_2\text{Ga}$  (**E**). Hence it appears that photoactivation of  $\text{Ga}(\mu\text{-CO})\text{Ga}$  results in the coordination of a second CO molecule at the expense of the Ga–Ga bond. On the other hand, exposure to visible light brings about the destruction of  $\text{Ga}(\mu\text{-CO})_2\text{Ga}$ , apparently with the regeneration of free CO and either Ga atoms or Ga<sub>2</sub> molecules.

(g) **In<sup>+</sup>OCCO<sup>-</sup>** (**J**). The last product remaining to be identified is **J**, the ultimate product of broad-band UV–visible photolysis of matrices formed by the co-deposition of indium vapor with CO. Its signature is a weak but sharp infrared absorption at the remarkably low frequency of 1515.5 cm<sup>-1</sup>. That this arises nevertheless from what is substantially a  $\nu(\text{C}-\text{O})$  mode is verified by the shift to 1482.6 cm<sup>-1</sup> brought about by replacement of <sup>12</sup>CO by <sup>13</sup>CO (calculated for a simple, uncoupled CO oscillator 1481.8 cm<sup>-1</sup>). With a mixture of <sup>12</sup>CO and <sup>13</sup>CO we observe a triplet pattern with the components at 1515.5/1513.5, 1490.0, and 1482.6 cm<sup>-1</sup> associated with the different <sup>12</sup>CO and <sup>13</sup>CO isotopomers.

Thompson and Jacox have investigated the products formed when an Ne/CO mixture is co-deposited with a beam of neon atoms that have been excited in a microwave discharge.<sup>39</sup> They observed a band at 1517.7 cm<sup>-1</sup> which shifted to 1484.5 cm<sup>-1</sup> when <sup>13</sup>CO was employed as the reagent gas and which they

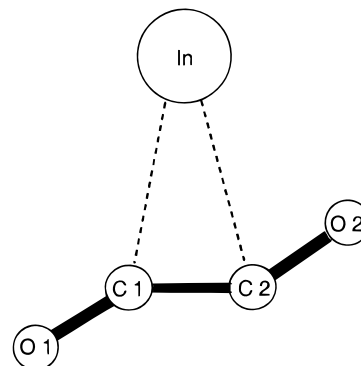


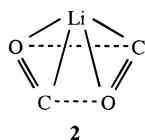
**Figure 15.** Calculated geometry ( $C_s$ ) for  $\text{In}^+[\text{C}_2\text{O}_2]^-$ . Bond lengths in Å: In–C1 2.613, In–C2 2.648, C1–C2 1.366, C1–O1 1.217, C2–O2 1.253. Bond angles in deg: C1–In–C2 30.1, O1–C1–C2 147.7, C1–C2–O2 146.0.

assigned to the  $\nu_{\text{asym}}(\text{C}-\text{O})$  mode of the  $\text{trans-OCCO}^-$  ion. Further experiments involving 1:1 mixtures of <sup>12</sup>CO and <sup>13</sup>CO led to the association of a feature at 1499.6 cm<sup>-1</sup> with the same mode in the ion  $\text{O}^{12}\text{C}^{13}\text{CO}^-$ . The close similarity of the frequencies we observe (1515.5 and 1482.6 cm<sup>-1</sup> for experiments involving <sup>12</sup>CO and <sup>13</sup>CO, respectively), allied to the pattern of the bands obtained using <sup>12</sup>CO/<sup>13</sup>CO mixtures, strongly suggests that **J** is  $\text{In}^+\text{OCCO}^-$  formed in all probability via a metal-to-ligand charge-transfer excitation of  $\text{In}(\text{CO})_2$ .

DFT calculations found a local minimum for  $\text{In}^+\text{OCCO}^-$  with a planar structure (see Figure 15). The two CO groups are trans to each other and the In is placed fairly symmetrically bridging the two carbon atoms. The two  $\nu(\text{C}-\text{O})$  modes have frequencies calculated to be 1795 and 1512 cm<sup>-1</sup>, with only the latter having significant intensity in IR absorption and therefore matching well the observed value. The C–C and C–O distances are similar to those predicted for the  $\text{OCCO}^-$  anion. The energy of this species is –60 kJ mol<sup>-1</sup> with respect to In and CO, so that it is 25 kJ mol<sup>-1</sup> less stable than  $\text{In}(\text{CO})_2$ .

The species  $\text{OCCO}^-$  has also been reported to be one of the numerous products formed on photolysis of CO-doped matrices

containing Na atoms.<sup>24</sup> Here it is reported that a perturbed  $\nu(\text{C}-\text{O})$  vibration of  $^{16}\text{O}^{12}\text{C}^{12}\text{C}^{16}\text{O}^-$  lies at  $1509\text{ cm}^{-1}$  and is shifted to  $1467\text{ cm}^{-1}$  when both  $^{12}\text{C}$  atoms are replaced by  $^{13}\text{C}$ . The use of mixtures containing  $^{12}\text{CO}$  and  $^{13}\text{CO}$  failed to identify any features attributable to the ion but calculations suggested that the two CO units behave as very weakly coupled oscillators such that the relevant vibrations of the mixed isotopomer are displaced but little from those of the parent compound. A species with bands occurring near  $1530\text{ cm}^{-1}$  has also been found in experiments where Li is co-condensed with CO in krypton matrices.<sup>25</sup> Again the effect of isotopic substitution is to bring about only a small perturbation of the bands due to the parent molecule. The species was identified as  $\text{Li}(\text{COCO})$  with the postulated structure **2**. The following assignments in the  $\nu(\text{C}-\text{O})$  region were made:  $^{12}\text{C}^{16}\text{O}^{12}\text{C}^{16}\text{O}^-$   $1532.8$  and  $1531.8\text{ cm}^{-1}$ ;  $^{13}\text{C}^{16}\text{O}^{13}\text{C}^{16}\text{O}^-$   $1501.0$  and  $1499.4\text{ cm}^{-1}$ ;  $^{12}\text{C}^{16}\text{O}^{12}\text{C}^{18}\text{O}^-$   $1529.0$  and  $1502.0\text{ cm}^{-1}$ . These are clearly consistent with the presence of two very slightly coupled CO oscillators. Although the formation of  $\text{LiOCCO}$  was also reported in the same studies, its identification with bands in the region of  $1720\text{--}1760\text{ cm}^{-1}$  suggests a much smaller degree of charge transfer than we observe for  $\text{In}^+\text{OCCO}^-$ .

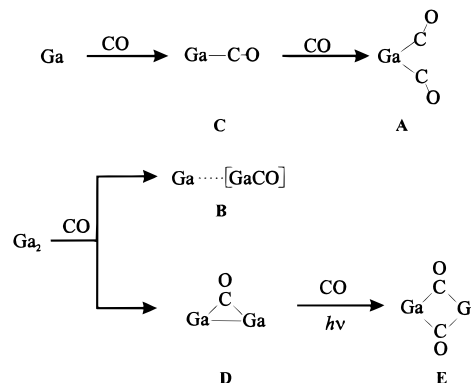


## 5. Conclusions

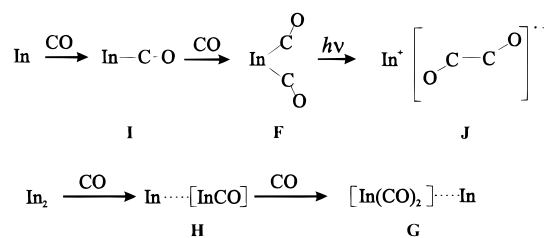
A matrix-isolation study has been carried out to explore the reactions that occur when gallium or indium vapors are co-condensed with carbon monoxide, and the resulting deposits are irradiated successively with UV ( $\lambda = 200\text{--}400\text{ nm}$ ) and broad-band UV-visible light ( $\lambda = 200\text{--}800\text{ nm}$ ). The various products have been identified and characterized by their infrared spectra. The response of the spectra to  $^{13}\text{CO}$  enrichment is the principal witness to the stoichiometries and likely structures, but evidence has also been sought from the effects of varying the concentrations of the reagents and from comparisons with the results of earlier studies of these or related systems. In addition, DFT calculations have been deployed to investigate the stabilities and geometries of the products and to simulate their vibrational properties so as to test the conclusions drawn from the experiments.

The products formed in the matrix were shown to be strongly dependent on the concentration of CO in the matrix. Our experiments then gave evidence that thermal or photochemical activation yielded the species  $\text{GaCO}$ ,  $\text{InCO}$ ,  $\text{Ga}\cdot\text{GaCO}$ ,  $\text{In}\cdot\text{InCO}$ ,  $\text{Ga}(\mu\text{-CO})\text{Ga}$ ,  $\text{Ga}(\text{CO})_2$ ,  $\text{In}(\text{CO})_2$ ,  $\text{In}(\text{CO})_2\cdot\text{In}$ ,  $\text{Ga}(\mu\text{-CO})_2\text{Ga}$ , and  $\text{In}^+\text{OCCO}^-$ . In the case of high CO concentrations (2%), the main event occurring initially on deposition of the matrices is the thermal reaction of the metal atoms M ( $\text{M} = \text{Ga}$  or  $\text{In}$ ) with an excess of CO to form the dicarbonyl species  $\text{M}(\text{CO})_2$  which evidently possess angular structures where the CO groups subtend an angle  $\theta$  of  $108^\circ$  and  $105^\circ$  for  $\text{M} = \text{Ga}$  and  $\text{In}$ , respectively. Quantum chemical calculations imply that the ground-state structures of these molecules feature narrow  $\text{C}-\text{M}-\text{C}$  angles and nonlinear  $\text{M}-\text{C}-\text{O}$  units oriented so that the CO groups are bent away from each other. The value of  $\theta$  thus calculated replicates closely that deduced experimentally for  $\text{Ga}(\text{CO})_2$ , but the agreement is distinctly less good for  $\text{In}(\text{CO})_2$ . The strong bands attributed to  $\text{In}(\text{CO})_2$  were accompanied by weaker features arising from a compound that also includes two equivalent terminal CO groups attached to the same In atom.

## SCHEME 1: Reaction Pathways for the Thermally and Photolytically Activated Reactions of Ga and Ga<sub>2</sub> with CO



## SCHEME 2: Reaction Pathways for the Thermally and Photolytically Activated Reactions of In and In<sub>2</sub> with CO



This product is probably a complex  $\text{In}(\text{CO})_2\cdot\text{In}$ , in which an  $\text{In}(\text{CO})_2$  molecule interacts with a neighboring In atom. Infrared bands which were weak at a CO concentration of 2% but dominated the spectra at a CO concentration of 0.2% have been identified with the monocarbonyls  $\text{MCO}$ . The  $\nu(\text{C}-\text{O})$  frequencies of such molecules increase in the order  $\text{AlCO} < \text{GaCO} < \text{InCO}$ , suggesting progressive weakening of the  $\text{M}-\text{CO}$  bond as the atomic number of M increases. Both of these features are borne out by earlier theoretical studies<sup>16</sup> and by the DFT calculations we have performed as part of the present work. Additionally, the monocarbonyls  $\text{M}\cdot\text{MCO}$ , the formation of which is also favored at low CO concentrations, were identified. Finally, the spectra obtained at low CO concentrations (0.2%) pointed to the formation of the monobridged species  $\text{Ga}(\mu\text{-CO})\text{Ga}$ . The properties of this and related species formed by the other group 13 metals (including the Al compound which has been observed previously<sup>12</sup>) have been explored by DFT methods.

Photoactivation with UV radiation leads to the formation of a new gallium carbonyl  $\text{Ga}(\mu\text{-CO})_2\text{Ga}$ , mainly at the expense of  $\text{Ga}(\mu\text{-CO})\text{Ga}$ . For this product a symmetrical  $D_{2h}$  structure incorporating two CO bridges is indicated both by experiment and by DFT calculations. It suffers decomposition under the action of visible radiation. Although UV radiation brings about the decay of all the indium carbonyls generated on deposition, no new product is evident until the matrix is exposed to broad-band UV-visible radiation. These conditions then give rise to low concentrations of a new species identified as  $\text{In}^+\text{OCCO}^-$ . In this case photoactivation of  $\text{In}(\text{CO})_2$  appears to have resulted in charge transfer with the coupling of two CO molecules to give the elusive  $\text{OCCO}^-$  carbanion. Calculations showed an increased electron density between the two carbon atoms in the first excited electronic state of  $\text{In}(\text{CO})_2$ , thereby lending support to the notion that  $\text{In}(\text{CO})_2$  is the precursor to  $\text{In}^+\text{OCCO}^-$  on irradiation at wavelengths between 200 and 800 nm.

Schemes 1 and 2 contrast the reaction pathways taken by Ga atoms and  $\text{Ga}_2$  molecules in the presence of CO with those taken



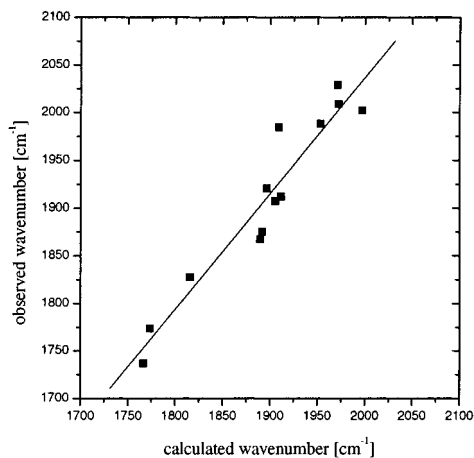


**Figure 16.** Comparison of the observed and calculated  $\nu(\text{C}-\text{O})$  frequencies for all the Al, Ga, and In carbonyls addressed in this work.

by In atoms and  $\text{In}_2$  molecules under similar (matrix) conditions. The frequencies of the  $\nu(\text{C}-\text{O})$  modes derived from DFT calculations are in satisfactory agreement with those determined experimentally. This is illustrated in Figure 16 where the observed frequencies are plotted versus the calculated ones for all Al, Ga, and In carbonyls which have been addressed in this work. A linear fit gives a line with a slope near 1 ( $1.2 \pm 0.1$ ,  $R = 0.957\ 61$ ).

**Acknowledgment.** The authors thank (i) the EPSRC for support of this research and for the award of an Advanced Fellowship to T.M.G., and (ii) the Deutsche Forschungsgemeinschaft for the award of a postdoctoral grant to H.-J.H.

## References and Notes

- (1) Wilkinson, G.; Stone, F. G. A.; Abel, E. W., Eds. *Comprehensive Organometallic Chemistry*; Pergamon Press: Oxford, UK, 1982. *Comprehensive Organometallic Chemistry II*; Pergamon Press: Oxford, UK, 1995.
- (2) Braterman, P. S. *Metal Carbonyl Spectra*; Academic Press: London, 1975.
- (3) See, for example: Geoffroy, G. L.; Wrighton, M. S. *Organometallic Photochemistry*; Academic Press: New York, 1979; Chapter 2.
- (4) See, for example: Hitam, R. B.; Mahmoud, K. A.; Rest, A. J. *Coord. Chem. Rev.* **1984**, *55*, 1–29. Almond, M. J.; Downs, A. J. *Adv. Spectrosc.* **1989**, *17*, 57–85.
- (5) Lembke, R. R.; Ferrante, R. F.; Weltner, W., Jr. *J. Am. Chem. Soc.* **1977**, *99*, 416–423.
- (6) Bos, A. J. *J. Chem. Soc., Chem. Commun.* **1972**, 26–27.
- (7) Slater, J. L.; Sheline, R. K.; Lin, K. C.; Weltner, W., Jr. *J. Chem. Phys.* **1971**, *55*, 5129–5130.
- (8) Hinchcliffe, A. J.; Ogdan, J. S.; Oswald, D. D. *J. Chem. Soc., Chem. Commun.* **1972**, 338–339.
- (9) Kasai, P. H.; Jones, P. M. *J. Am. Chem. Soc.* **1984**, *106*, 8018–8020. Chenier, J. H. B.; Hampson, C. A.; Howard, J. A.; Mile, B.; Sutcliffe, R. *J. Phys. Chem.* **1986**, *90*, 1524–1528.
- (10) Chenier, J. H. B.; Hampson, C. A.; Howard, J. A.; Mile, B. *J. Chem. Soc., Chem. Commun.* **1986**, 730–732.
- (11) Chertikhin, G. V.; Rochanskii, I. L.; Serebrennikov, L. V.; Shevel'kov, V. F. *Russ. J. Phys. Chem. (Engl. Transl.)* **1988**, *62*, 1165–1167.
- (12) Xu, C.; Manceron, L.; Perchard, J. P. *J. Chem. Soc., Faraday Trans.* **1993**, *89*, 1291–1298.
- (13) Feltrin, A.; Guido, M.; Nunziante Cesaro, S. *Vib. Spectrosc.* **1995**, *8*, 175–183.
- (14) Balaji, V.; Sunil, K. K.; Jordan, K. D. *Chem. Phys. Lett.* **1987**, *136*, 309–313. Sunil, K. K.; Bolkovac, P. M.; Jordan, K. D. In *Gas-Phase Metal Atom Reactions*; Fontijn, A., Ed.; Elsevier: Amsterdam, 1992.
- (15) McQuaid, M.; Woodward, J. R.; Gole, J. R. *J. Phys. Chem.* **1988**, *92*, 252–255.
- (16) Bridgeman, A. J. *J. Chem. Soc., Dalton Trans.* **1997**, 1323–1329.
- (17) Hamrick, Y. M.; Van Zee, R. J.; Godbout, J. T.; Weltner, W., Jr.; Lauderdale, W. J.; Stanton, J. F.; Bartlett, R. J. *J. Phys. Chem.* **1991**, *95*, 2840–2844, 5366.
- (18) Burkholder, T. R.; Andrews, L. *J. Phys. Chem.* **1992**, *96*, 10195–10201.
- (19) Howard, J. A.; Sutcliffe, R.; Hampson, C. A.; Mile, B. *J. Phys. Chem.* **1986**, *90*, 4268–4273.
- (20) Kasai, P. H.; Jones, P. M. *J. Phys. Chem.* **1985**, *89*, 2019–2021.
- (21) Ogdan, J. S. In *Cryochemistry*; Moskovits, M., Ozin, G. A., Eds.; Wiley: New York, 1976; p 247.
- (22) Hatton, W. G.; Hacker, N. P.; Kasai, P. H. *J. Phys. Chem.* **1989**, *93*, 1328–1332.
- (23) Ayed, O.; Loutellier, A.; Manceron, L.; Perchard, J. P. *J. Am. Chem. Soc.* **1986**, *108*, 8138–8147. Silvi, B.; Ayed, O.; Person, W. B. *J. Am. Chem. Soc.* **1986**, *108*, 8148–8153.
- (24) Ayed, O.; Manceron, L.; Silvi, B. *J. Phys. Chem.* **1988**, *92*, 37–45.
- (25) Krishnan, C. N.; Hauge, R. H.; Margrave, J. L. *J. Mol. Struct.* **1987**, *157*, 187–196.
- (26) See, for example: Church, S. P.; Poliakoff, M.; Timney, J. A.; Turner, J. *J. Inorg. Chem.* **1983**, *22*, 3259–3266.
- (27) Baerends, E. J.; Berces, A.; Bo, C.; Boeringer, P. M.; Cavallo, L.; Deng, L.; Dickson, R. M.; Ellis, D. E.; Fan, L.; Fischer, T. H.; Fonseca Guerra, C.; van Gisbergen, S. J.; Groeneveld, J. A.; Gritsenko, O. V.; Harris, F. E.; van den Hoek, P.; Jacobsen, H.; van Kessel, G.; Kootstra, F.; van Lenthe, E.; Osinga, V. P.; Philipsen, P. H. T.; Post, D.; Pye, C. C.; Ravenek, W.; Ros, P.; Schipper, P. R. T.; Schreckenbach, G.; Snijders, J. G.; Sola, M.; Swerhone, D.; te Velde, G.; Vernooijs, P.; Versluis, L.; Visser, O.; van Wezenbeek, E.; Wiesenekker, G.; Wolff, S. K.; Woo, T. K.; Ziegler, T. ADF Program System Release 2.3, 1997.
- (28) Fonseca Guerra, C.; Snijder, J. G.; te Velde, G.; Baerends, E. J. *Theor. Chem. Acc.* **1998**, *99*, 391–403.
- (29) Vosko, S. H.; Wilk, L.; Nusair, M. *Can. J. Phys.* **1980**, *58*, 1200–1211.
- (30) Becke, A. D. *Phys. Rev.* **1988**, *A38*, 3098–3100.
- (31) Perdew, J. P. *Phys. Rev.* **1986**, *B33*, 8822–8824.
- (32) Fan, L. Y.; Ziegler, T. *J. Phys. Chem.* **1992**, *96*, 6937–6941.
- (33) Fan, L. Y.; Ziegler, T. *J. Chem. Phys.* **1992**, *96*, 9005–9012.
- (34) Dubost, H. *Chem. Phys.* **1976**, *12*, 139–151.
- (35) Downs, A. J., Ed. *Chemistry of Aluminium, Gallium, Indium and Thallium*; Blackie: Glasgow, UK, 1993.
- (36) Büchner, W. *Helv. Chim. Acta* **1963**, *46*, 2111–2120.
- (37) Büchner, W. *Helv. Chim. Acta* **1966**, *49*, 907–913.
- (38) Guglielminotti, E.; Coluccia, S.; Garrone, E.; Cerruti, L.; Zecchina, A. *J. Chem. Soc., Faraday Trans. 1* **1978**, *75*, 96–108.
- (39) Thompson, W. E.; Jacox, M. E. *J. Chem. Phys.* **1991**, *95*, 735–745.